Numerical study of oxide thin film growth by using Nd:YAG laser beam

J.L. Jiménez-Pérez
CICATA-IPN. Legaria 694, Col. Irrigación, 11500 México D. F., México

P.H.Sakanaka
Departamento de Física Quántica. Instituto de Física "Gleb Wataghin" Universidade Estadual de Campinas, 13083-970 Campinas, S.P. Brazil

M.A. Algatti
Departamento de Física e Química, Universidade Estadual Paulista "Julio de Mesquita Filho", Campus de Guaratinguetá 12500-000 Guratinguetá, S.P., Brazil

A. Cruz-Orea[d], J.G. Mendoza-Alvarez
Departamento de Física, CINVESTAV-IPN, A. P. 14-740 , 07300 México D.F., México

N. Muñoz-Aguirre
Instituto Méxicano del Petroleo, México D.F., México.

Based on a previous developed and published one-dimensional model for the growth of metallic oxide thin films, we have studied the tridimensional growth rates for titanium dioxide films grown on Ti layers. The thermo-oxidation process of Ti films, deposited over glass substrates, is due to the film surface heating occurring when an intense beam of a pulsed Nd:YAG laser moves at constant speed on the surface exposed to air. The computational algorithm used for the calculations in this model takes into account self-consistently the heat flux equation, the Gaussian-shape laser beam, and the parabolic oxidation law starting with the initial values of the heating parameters. From these calculations we obtained a tridimensional picture of film morphology. The theoretical estimations of the film thickness and the growth ratio show excellent agreement with the measured experimental values.

Keywords: Laser induced oxidation; Thin oxide films; Laser materials processing

1. Introduction

The great advantage of using pulsed laser sources for materials processing is that it is posible to heat an extremely well localized region without affecting the properties of the surrounding environment. As an example of such versatility we can mention the thermo-chemical oxidation of thin metallic surfaces of Ti on $NbLiO_3$ substrates for micro-waveguide fabrication [1-6]. Thermo-chemical modification of Ti films and other materials are widely used for optical recording and deposition of masking layers [7,8]. In the above-mentioned applications it is very difficult to solve analytically the film's growth rate equation which cannot be decoupled from the heat diffusion equation. Taking into account our operation condition (thermo-oxidation reaction induced by one incident laser over a metallic surface exposed to air), we know that for metallic oxidation the oxide film growth follows a parabolic law [9]. For these specific growth conditions we study spatial geometry of the titanium dioxide film formed on the Ti metallic film surface deposited on a glass slide, which moves at constant speed in front of the laser beam. Inspecting the relief of the traces we can observe the dependence of this on the operational parameters. Furthermore, we study the temporal evolution of the film thickness and its maximum value and their dependence on laser parameters. The calculated results of our model are compared with available experimental measurements [10].

2. Temperature Distribution and Film Growth.

Our model is based on a self-consistent numerical solution of one problem described as follows. When the laser beam heats a metallic film surface exposed to air, an oxidation process takes place, which initiates the oxide film growth. This film is considered thermally thin. This layer then changes the optical (reflectivity, refractive index, etc.) and thermal (thermal conductivity, diffusivity, etc.) properties which also changes the temperature distribution, and consequently the rate of oxidation. Taken into account these last considerations we can predict the interface metal-oxide temperature T(x,y,z,t) and relate it with the oxide film rate growth in the parabolic regime as follows [9,11].

First we solve the heat flux equation:

$$r_j(T)C_j(T)\left(\frac{\partial T_j}{\partial t}\right) = \nabla(k_j(T)\nabla T_j) + F_j(\vec{r},t) \qquad (1)$$

where ñ$_j$(T), C_j(T), ê$_j$(T) and T_j are the temperature dependent density, heat capacity, heat conductivity and also temperature of the j-th material. j=1 refers to the metallic film, and j=2 refers to the glass substrate. The heating source is described by a Gaussian-like shape:

$$F_1(\bar{r},t) = a\, I(t) A(l) \exp\left\{ \frac{-(x - v_x t)^2 - y^2}{w^2{}_0} - a\, z \right\} \quad (2)$$

where á, í$_x$ and ù$_0$ are the optical absorption coefficient, the scanning speed and the laser beam spot size, respectively.

This model considers the parabolic law of oxidation for the oxide film thickness *l* [11]:

$$\frac{dl}{dt} = \frac{d_0}{l} \exp\left\{ -\frac{T_D}{T_1(x, y, z, t)} \right\} \quad (3)$$

Where d_0 and T_D are thermodiffusive constants.

And the beam intensity is given by [9]:

$$I(t) = I_0 t_0 \sum_{m=0}^{\infty} d\,(t - mt) \quad (4)$$

Where I_0, $\hat{o}_0$ and $\hat{o}^{-1}$ are the peak intensity, the pulse width and repetition frequency of the laser beam, respectively.

The δ function can be represented by:

$$d(t - mt) = \frac{1}{\sqrt{p t^2{}_0}} \int_{-\infty}^{+\infty} e^{\frac{-(t-mt)^2}{t^2{}_0}} dt \quad (5)$$

And the absorptivity of the layered metal-oxide film of thickness l, A(l) is given by:

$$A(l) = 1 - |R(l)|^2 \quad (6)$$

where R(*l*) is the reflectivity of the layered metal-oxide film. For the case of normal incidence we have [12]

$$R(l) = \frac{r_{12} e^{-2iy} + r_{23}}{e^{-2iy} + r_{12} r_{23}} \quad (7)$$

where

$$r_{12} = \frac{1 - \sqrt{e}}{1 + \sqrt{e}} \quad (8)$$

$$r_{23} = \frac{r_{12} - r_{13}}{r_{12} r_{13} - 1} \quad (9)$$

$$r_{13} = \sqrt{1 - A_0} \quad (10)$$

and

$$y = \frac{2pn l \sqrt{e}}{c} \quad (11)$$

where í is the laser radiation frequency r_{12} and r_{13} are the amplitude reflection coefficients from the oxide and from the metal, respectively, A_0 is the absorptivity of the metal without the oxide film. The dielectric constant is given by å$^{1/2}$=*n*+*ik* where *n* and *k* are the refractive index and the extinction coefficient for the oxide.

The numerical solution of the equation 1 took into account the following boundary conditions:

$$T_1(x, y, z, 0) = T_2(x, y, z, 0) = T_E \quad (12)$$

Where T_E is the environment temperature

$$\frac{\partial T_j(0, y, z, t)}{\partial x} = \frac{\partial T_j(x_0, y, z, t)}{\partial x} = 0 \quad (13)$$

$$\frac{\partial T_j(x, 0, z, t)}{\partial y} = \frac{\partial T_j(x, y_0, z, t)}{\partial y} = 0 \quad (14)$$

being x_0 and y_0 the substratum length and width respectively. Here j=1 corresponds to the metal and j=2 to the glass substratum. The boundary conditions at the film-substratum interface are:

$$k_1 \frac{\partial T_1(x, y, z_1, t)}{\partial z} = k_2 \frac{\partial T_2(x, y, z_1, t)}{\partial z} \quad (15)$$

and

$$T_1(x, y, z_1, t) = T_2(x, y, z_1, t) \quad (16)$$

being z_1 the thickness of the metallic film. The heat flux at the substratum base (z = z_b) is equal zero, i.e.:

$$k_2 \frac{\partial T_2(x, y, z_b, t)}{\partial z} = 0 \quad (17)$$

The thickness *l*(x,y,0,t) is obtained from the numerical integration of Eq. 3 with T(x,y,0,t) numerically obtained from an self-consistent procedure. This permits us to measure $l_{máx}$, which is the maximum value of the oxide formed on the metallic film for different incident intensities. This also permits to carry out probes of the trace profiles as a function of the operational parameters.

3. Experiment

The growth of the TiO_2 films was performed on Ti thin films(Thickness of ~1000Å) deposited on microscope glass slides by the evaporation method, the oxidation of Ti was obtained using a Nd:YAG laser with λ=1.06 µm, pulse with 290 ns at FWHM, repetition rate of 201Hz, and v_x=2 mm/s (scanning speed of laser beam spot size) operating in

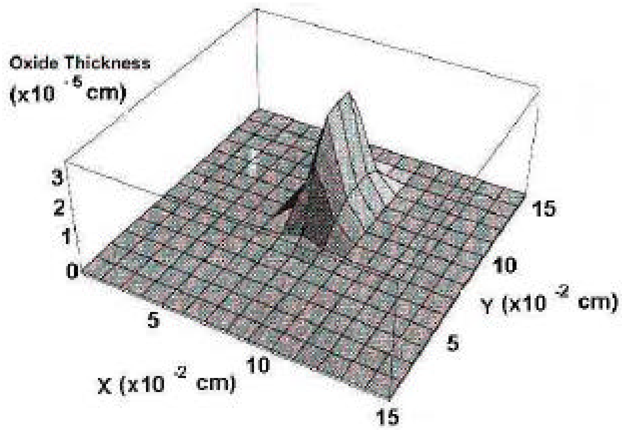

Figure 1. Space profile of titanium dioxide thickness for the pulsed laser beam. The pulse repetition frequency is 200 Hz, the number of pulses is 200 and the pulse duration is 290 ns. The laser scanning speed was kept fixed in 2 mm/s.

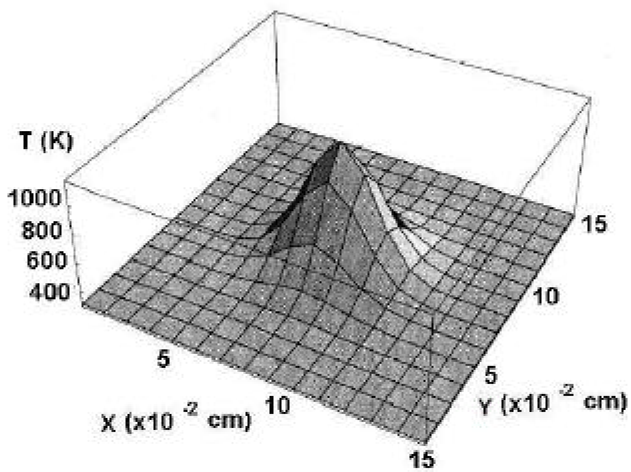

Figure 2. Space profile of the surface temperature for the laser beam parameters presented in figure 1.

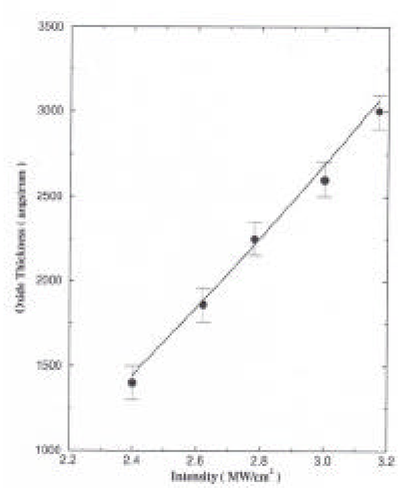

Figure 3. Oxide thickness dependence on laser intensity for 200 laser pulses (τ = 290 ns, f = 200 Hz, v_x= 2 mm/s). The full line corresponds to theoretical values, and the dots to the experimental data.

film target. The laser pulses were focused on the samples by a specially built optical system consisting of a combination of an expander and an objective with a focal length forming a beam radius of 1mm (at 1/e point from the maximum intensity) in the focal plane. The total growth thickness of oxide films by 100 consecutive pulses was measured using a microprofilometer Tencor Alpha-Step 100^{TM} with an accuracy of 10 Å. The chemical composition of the tracks was determined from micro-Raman spectra of the samples measured using the 514.5 nm line of an Ar^+ ion laser (Coherent 90-5), operating in the power range from 300 to 400 mW. The sample's micro-Raman spectra results showed two strong bands at 424 cm^{-1} and 612 cm^{-1} associated to the rutile TiO_2 structure, which confirmed that the experimental conditions favored this oxide stoichiometry.

4. Results and Discussions

In Fig. 1, we show the self-consistent spatial profile calculated from the micro-located trace of metallic oxide formed by the exposition of a Ti film to a laser beam. For this case we consider a Titanium film with a thickness of ~1000 Å deposited on a glass substrate of 1mm thickness exposed to one sequence of 200 pulses from a Nd: YAG laser beam (λ=1.06 μm). From the space profile of the oxide track for the laser beam characteristics presented in this figure it may be seen that the track profile closely matches the laser beam space profile. The maximum calculated value for the oxide thickness was around 3000 Å.

The corresponding temperature distribution at the oxide-metal interface is shown in Fig. 2. In both cases; the figures represent instantaneous pictures of the situation after one second of time exposure to the pulses that are emitted at 200 Hz beam frequency and the sample scanning velocity was 2 mm/s. The individual beams are pulse trains with a temporal width of 290 n. The maximum calculated temperature for the oxide-metal interface was around 1200 K.

Finally, in Fig. 3 we show the behavior of the maximal oxide thickness *l* after *t = 1s* as a function of the laser intensity. These values were taken at the maximum oxide thickness for each laser intensity. The dot symbols represent the experimental measurements taken with the profilometer and the continuous line represent the theoretical results obtained from our self-consistent calculations. It can be seen that the oxide thickness increases monotonically as the laser peak intensity varies from 2.4 to 3.17 MW/cm^2. The theoretical curve resulted from the integration of equation (3), is in close agreement with the experimental data.

5. Conclusions

In summary, in this paper we have shown results on the calculation of the tridimensional profile of a titanium dioxide thin film grown by the oxidation of a Ti film produced by the irradiation with a Gaussian-like laser beam. Using a self-consistent model which takes into account the heat flux equation, the parabolic law of oxidation and a Gaussian-like laser beam shape, we calculated the tridimensional temperature distribution and thickness distribution profiles for a given set of parameter values. By comparing the theoretical results for the TiO_2 film thickness predicted by our model with the experimental values from profilometer measurements we demonstrated a very good agreement, which show the correctness of our self-consistent model to describe this type of film growth process. It also should be pointed out that such control of the experimental parameters is necessary for the use of this technique in microlitography process where high accuracy pattering capability is of key importance.

Acknowledgements

We acknowledge the partial financial support of Conacyt-Mexico, Cegepi-Cofaa-IPN-Mexico, and CNPq-Brasil.

References

[1] S. Zhu, Y.F. Lu, M.H. Hong, and X.Y. Chem, J. Appl. Lett., **89**, 2400 (2001).
[2] D. Ramanathan and P.A. Molian, Appl. Phys. Lett. **78**, 1484 2001).
[3] P.R. Willmatt and J. Huber, Rev. Mod. Phys., **72**, 315 (2000).
[4] M. Haruna, Y. Murata, H. Nishihara, Jpn. J. Appl. Phys. **31**, 1593 (1992).
[5] B. Haba, B.W. Hussey, A. Gupta, J. Appl. Phys. **69**, 2871 (1991).
[6] A. Ferrari, L. Shirone, G. Maiello, C. de Cesare, F. Carassitti, M. Bertolotti, M.A. Caparonero, A. Luches, M. Martino, M. Dinescu, N. Chitica, I.N. Mihailescu, I. Ursu, J. Mod. Opt. **40**,1043 (1993).
[7] R. Winn Hardin, "Rings reveal details on ultrafast ablations", Laser Focus World, August **15,** (1998).
[8] Philippe Bado, "Ultrafast pulses create waveguides and microchannels", Laser Focus World, April, **73,** (2000).
[9] M.I. Arzuov, F.V. Bunkin, N.A. Kirichenko, V.J. Konov, B.S. Luk`yanchuk, JETP Lett. **27**, 215 (1978).
[10] J.L. Jiménez Pérez, P.H. Sakanaka, M.A. Algatti, J.G. Mendoza-Alvarez and A. Cruz-Orea, Appl. Surf. Sci., **175**, 709 (2001).
[11] M.I. Arzuov, F.V. Bunkin, N.A. Kirichenko, V.J. Konov, B.S. Luk`yanchuk, Sov. Tech. Phys. Lett. **5**, 76 (1979).
[12] M.I. Arzuov, A. I. Barchukov, F.V. Bunkin, N.A. Kirichenko, V.J. Konov, B.S. Luk`yanchuk, Sov. J. Quantum Electron. **9(3)**, 281 (1979).